IL NUOVO CIMENTO Vol. 26 C, N. 5 Settembre-Ottobre 2003
DOI 10.1393/ncc/i2002-10002-6

Domain of validity of some atmospheric mesoscale models

M. A. Nuñez(*)

Departamento de Física, Universidad Autonoma Metropolitana Iztapalapa
Apartado Postal 55-534, C.P. 09340 México, Distrito Federal, México

(ricevuto il 15 Febbraio 2002; revisionato il 15 Settembre 2003; approvato il 19 Novembre 2003)

Summary. — The usual coordinate system in the mesoscale literature is a Cartesian system xyz with its origin at a point on a spherical earth model with the z-axis normal and exterior to the earth. The main form of the momentum equation for theoretical analysis has been $\mathrm{d}\mathbf{v}/\mathrm{d}t = -\rho^{-1}\boldsymbol{\nabla}\, p + \mathbf{g} - 2\vec{\Omega} \times \mathbf{v} + \mathbf{f}_r$ where $\mathbf{g}$ is approximated by $-g\hat{\mathbf{z}}$. Several computational models use a version of this equation where z is replaced by a σ-type coordinate, and applications of such models have used a horizontal domain $\mathcal{D}(L) = 2L \times 2L$ with $L \gtrsim 650$ km but the results of this paper suggest that the equation is valid with $L \lesssim 100$ km. However, the necessity of including the effects of synoptic disturbances and reducing the errors from lateral boundaries impose the use of a large $\mathcal{D}(L)$. This conflict is solved with the use of the correct gravitational acceleration $\mathbf{g} = -ga^2\mathbf{R}r^{-3}$ which provides a momentum equation valid on any domain $\mathcal{D}(L)$. This is confirmed with an example which shows that the resulting momentum equation can yield the correct pressure field on the whole earth surface. Practical problems limit the use of the coordinate system xyz to $L \lesssim 500$ km. In this case, it is shown that the approximation $\mathbf{g} \sim -g(x\hat{\mathbf{x}} + y\hat{\mathbf{y}} + a\hat{\mathbf{z}})/a$ can be applied. Some mesoscale models incorporate map projections into model equations to consider the earth curvature. This has motivated the use of such models on a domain with $L \sim 882$, 1665 km. Formally, the governing equations from map projections are written in terms of a curvilinear coordinate system $x_p y_p z_p$ but it is shown that if x_p, y_p, z_p are taken as x, y, z the resulting momentum equation is valid on a region with $L \lesssim 100$ km.

PACS 92.60.Wc – Weather analysis and prediction.
PACS 92.60.Sz – Air quality and air pollution.

(*) E-mail: manp@xanum.uam.mx

1. – Introduction

The fundamental momentum vector equation for an air parcel in any coordinate system fixed to the earth is

$$\frac{\mathrm{d}\mathbf{V}}{\mathrm{d}t} = -\frac{1}{\rho}\boldsymbol{\nabla}\, P + \mathbf{g} - 2\vec{\Omega} \times \mathbf{V} + \mathbf{f}\,, \tag{1.1}$$

where $\mathbf{V}$, ρ, P are the velocity vector, density and pressure, respectively, $\vec{\Omega}$ is the earth's angular velocity, $\mathbf{f}$ is a frictional force and terms with Ω^2 are neglected. If we consider a uniform-mass spherical earth, the gravitational acceleration is given by

$$\mathbf{g} = -g\frac{a^2}{r^3}\mathbf{R} \tag{1.2}$$

with $g \equiv GMa^{-2}$, $\mathbf{R}$ being the vector from the earth's center to the parcel, $r = \|\mathbf{R}\|$, M and a are the mass and radius of the earth and G is the gravitational constant [1]. As a result of relatively small horizontal scales of mesoprocesses, mesometeorological problems do not as a rule involve the use of a spherical coordinate system or, in general, any system which account for the earth's curvature [2]. The usual coordinate system in the standard mesoscale literature is a Cartesian system xyz with its origin at a point P_c in latitude ϕ_c on the terrestrial sphere, the (x, y)-plane is normal to $\mathbf{g}$ at P_c and the z-axis is outside of the earth [2-12]. It is generally acknowledged that when the horizontal scale of the motion L ($|x|, |y| \leq L$) is of order 10^3 km or smaller, the gravitational acceleration $\mathbf{g}$ can be taken as a constant and normal to the (x, y)-plane [7]. Thus, the most common form of the momentum equation used in the mesoscale literature [2-12] is

$$\frac{\mathrm{d}\mathbf{v}}{\mathrm{d}t} = -\frac{1}{\rho}\boldsymbol{\nabla}\, p - g\hat{\mathbf{z}} - 2\vec{\Omega} \times \mathbf{v} + \mathbf{f}, \tag{1.3}$$

where $\hat{\mathbf{z}}$, $\hat{\mathbf{x}}, \hat{\mathbf{y}}$ are the unit vectors of the xyz-system. This is a simple equation to perform theoretical analyses with the effects of rotation included, which has been used by numerical mesoscale models to treat problems with complex topography. In this latter case the z-coordinate is replaced by either a σ_z- or σ_p-coordinate to simplify the treatment of lower boundary conditions [5, 6, 10, 13]. Following this scheme, several mesoscale computational systems that solve (1.3) in coordinates $xy\sigma_z$ or $xy\sigma_p$ have been developed [13-15]. Although some authors have pointed out that the range of validity of eq. (1.3) may be very small [16, 1], some applications of these computational systems to air pollution studies [17] have considered a horizontal domain $\mathcal{D}(L) = 2L \times 2L$ with $L \gtrsim 650$ km but the results of this paper suggest that eq. (1.3) is valid on a region $\mathcal{D}(L^0_{\max})$ with $L^0_{\max} \lesssim 100$ km.

Two problems motivate the use of a large horizontal domain $\mathcal{D}(L)$. The first is the necessity of including the influence of propagating synoptic disturbances on the regional weather; for instance, Pielke suggests a domain of at least 5000 km on a side to reasonably resolve some disturbances in winter [13, p. 445]. The second is that the boundary errors induced by artificial boundaries (which are unavoidable in limited-area numerical models) do not contaminate the results with a large $\mathcal{D}(L)$. The solution of these problems is incompatible with the small domain of validity $\mathcal{D}(L^0_{\max})$ of the numerical models that solve (1.3) in $xy\sigma$-coordinates [13-15]. The answer to this conflict is the use of the

TABLE I. – *Magnitudes in* ms^{-2} *of terms in the u-equation for flows with horizontal scale L* (m), $U = 10\ \mathrm{ms}^{-1}$, $H = 10^4$ m, $f = 2\Omega \sin\phi$, $\phi = 45^\circ$, $g = 10\ \mathrm{ms}^{-2}$ [9], *and* $x = L/2$, $y = z = 0$, $r = \sqrt{x^2 + a^2}$, $a = 6378$ km.

	$\mathrm{d}u/\mathrm{d}t =$	$-\frac{1}{\rho}\frac{\partial p}{\partial x}$	$+fv$	$-fw$	$+\frac{\partial}{\partial z}K_z\frac{\partial u}{\partial z}$	$+\frac{\partial}{\partial x}K_H\frac{\partial u}{\partial x}$	$-\frac{ga^2x}{r^3}$
L	U^2/L	$\Delta P/\rho L$	fU	fHU/L	KU/H^2	KU/L^2	
10^6	10^{-4}	10^{-3}	10^{-3}	10^{-5}	10^{-6}	10^{-10}	10^{0}
10^5	10^{-3}	10^{-2}	10^{-3}	10^{-4}	10^{-6}	10^{-8}	10^{-1}
10^4	10^{-2}	10^{-1}	10^{-3}	10^{-3}	10^{-6}	10^{-6}	10^{-2}

exact gravity acceleration (1.2). If a parcel is at the point (x, y, z) at time t we have $\mathbf{R} = x\hat{\mathbf{x}} + y\hat{\mathbf{y}} + (z + a)\hat{\mathbf{z}}$ and the correct momentum equation is

$$\frac{\mathrm{d}\mathbf{v}}{\mathrm{d}t} = -\frac{1}{\rho}\boldsymbol{\nabla}\, p - g\frac{a^2}{r^3}[x\hat{\mathbf{x}} + y\hat{\mathbf{y}} + (z + a)\hat{\mathbf{z}}] - 2\vec{\Omega} \times \mathbf{v} + \mathbf{f}, \tag{1.4}$$

whose numerical implementation requires a small modification of the numerical mesoscale software developed to the date. Some authors consider that the coordinate system xyz is not well suited for practical applications to large-scale problems, in part, because the latitudinal variation of the Coriolis force has to be included and a large-scale flow will fall below the tangent plane and acquire a z-component in the xyz-system [16, 1, 7]. However, the vector equation (1.1) is valid for *any* coordinate system rotating with the earth [1] and this includes the xyz-system. Thus, in strict mathematical terms, eq. (1.4) together with the conservation equations of mass, energy, moisture and the equation of state, provides the correct meteorological fields when the correct initial and boundary conditions are used, independently of the magnitude of the domain $\mathcal{D}(L)$. This is illustrated in subsect. **3**˙1, where a simple problem shows that eq. (1.4) can yield the correct pressure field on the *whole* earth.

Map projections have been used in atmospheric modeling with the purpose of including the earth sphericity into model equations [6, 18, 19]. Accordingly, some mesoscale computational systems that use coordinates $xy\sigma_z$ [20] or $xy\sigma_p$ [21] include metric factors in the horizontal derivatives of model equations to consider map projections. This has motivated the use of such computational systems on horizontal domains $\mathcal{D}(L)$ with L as large as 885 km [22] or 1665 km [23]. In principle, the use of map projections generates orthogonal coordinate systems $x_p y_p z_p$ which are legitimate to solve model equations. However, in sect. **4** it is shown that if x_p, y_p, z_p are taken as correct approximations of x, y, z, respectively, the horizontal momentum equations omit the gravitational acceleration and, therefore, their reliability region is similar to $\mathcal{D}(L^0_{\max})$. Following Atkinson [9], table I yields the magnitude of the terms in the u-equation, where the term ga^2xr^{-3} was added, for a flow with horizontal length scale L (m), $U = 10\ \mathrm{ms}^{-1}$, $H = 10^4$ m, $g = 10\ \mathrm{ms}^{-2}$, $a = 6378$ km, $\phi = 45^\circ$ and $x = L/2$, $y = z = 0$. For flows with L from 10^5 to 10^6 m the term ga^2xr^{-3} is dominant while the dissipative terms are very small, so that the latter will be ignored in the next sections.

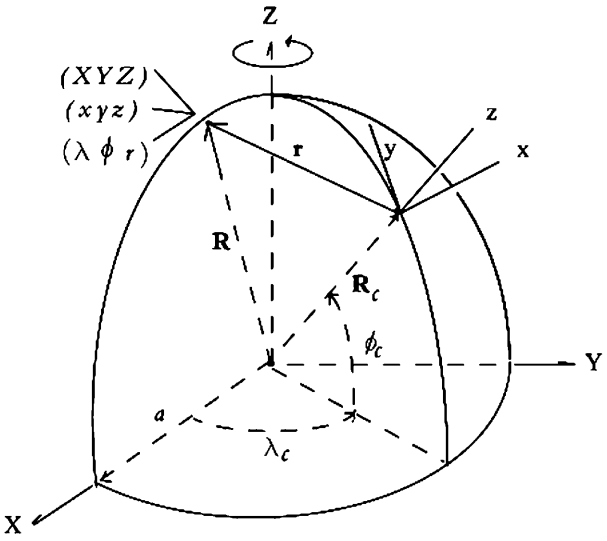

Fig. 1. – Reference systems XYZ, xyz, spherical coordinates $\lambda\phi r$ and position vectors $\mathbf{R}$, $\mathbf{r}$ of a parcel.

2. – Governing equations for dry and inviscid air

Consider a spherical earth with uniform mass. The primary Cartesian coordinate system XYZ is defined with its origin at the earth's center, is fixed to the earth and the Z-axis coincides with the earth's rotation axis, as shown in fig. 1. If $\hat{\mathbf{X}}, \hat{\mathbf{Y}}, \hat{\mathbf{Z}}$ are unitary vectors on the positive X, Y, Z axes and $\mathbf{R} = X\hat{\mathbf{X}} + Y\hat{\mathbf{Y}} + Z\hat{\mathbf{Z}}$ is the position vector of an air parcel with mass m, the gravitational force on m is

$$\mathbf{f}_{\mathrm{g}} = -GMm\frac{\mathbf{R}}{r^3} = -g\frac{a^2}{r^3}m\mathbf{R}\,, \qquad g \equiv \frac{GM}{a^2}\,, \tag{2.1}$$

where r is the magnitude of $\mathbf{R}$, M and a are the mass and radius of the earth and G is the gravitational constant. Let $\mathbf{V} = \mathrm{d}\mathbf{R}/\mathrm{d}t$ and consider that the flow is inviscid, then the momentum equation of a parcel in the XYZ system is

$$\frac{\mathrm{d}\mathbf{V}}{\mathrm{d}t} + 2\vec{\Omega}\times\mathbf{V} + \vec{\Omega}\times(\vec{\Omega}\times\mathbf{R}) = -\frac{1}{\rho}\boldsymbol{\nabla}\, P - g\frac{a^2}{r^3}\mathbf{R}\,,$$

where ρ and P are the density and pressure and $\vec{\Omega} = \Omega\hat{\mathbf{Z}}$ is the earth angular velocity [1]. If we set $\mathbf{V} = U\hat{\mathbf{X}} + V\hat{\mathbf{Y}} + W\hat{\mathbf{Z}}$ and neglect the term $\vec{\Omega}\times(\vec{\Omega}\times\mathbf{R})$, the governing equations are

$$\begin{aligned}
\frac{\mathrm{d}U}{\mathrm{d}t} - 2\Omega V &= -\frac{1}{\rho}\frac{\partial P}{\partial X} - g\frac{a^2}{r^3}X\,,\\
\frac{\mathrm{d}V}{\mathrm{d}t} + 2\Omega U &= -\frac{1}{\rho}\frac{\partial P}{\partial Y} - g\frac{a^2}{r^3}Y\,,\\
\frac{\mathrm{d}W}{\mathrm{d}t} &= -\frac{1}{\rho}\frac{\partial P}{\partial Z} - g\frac{a^2}{r^3}Z,
\end{aligned} \tag{2.2a}$$

and $P = \mathcal{R}T\rho$,

$$\frac{\mathrm{d}\log\rho}{\mathrm{d}t} + \frac{\partial U}{\partial X} + \frac{\partial V}{\partial Y} + \frac{\partial W}{\partial Z} = 0, \qquad c_p\rho\frac{\mathrm{d}T}{\mathrm{d}t} = \frac{\mathrm{d}P}{\mathrm{d}t}, \tag{2.2b}$$

where T is the temperature, $\mathcal{R}$ is the gas constant and $\mathrm{d}/\mathrm{d}t = \partial/\partial t + U(\partial/\partial X) + V(\partial/\partial Y) + W(\partial/\partial Z)$.

To define the system xyz on a plane tangent to the earth, we consider that the location of a point on the terrestrial sphere is given by the latitude ϕ and longitude λ, as fig. 1 shows, where ϕ is positive on the north hemisphere, the reference meridian is on the (x, z)-plane and λ is positive eastward. The coordinate system xyz has its origin at a point (λ_c, ϕ_c), the x (y)-axis is tangent to the parallel circle (meridian) at (λ_c, ϕ_c), is positive eastward (northward), and the z-axis is taken out of the earth. If $\hat{\mathbf{x}}, \hat{\mathbf{y}}, \hat{\mathbf{z}}$ are the unit vectors on the positive xyz-axes, the position vector of a parcel at the point (x, y, z) is $\mathbf{r} = x\hat{\mathbf{x}} + y\hat{\mathbf{y}} + z\hat{\mathbf{z}}$. From the equation $\mathbf{R} = \mathbf{r} + \mathbf{R}_c$ we get the relation between the coordinates XYZ and xyz,

$$\begin{pmatrix} x \\ y \\ z + a \end{pmatrix} = \mathbb{R}_c \begin{pmatrix} X \\ Y \\ Z \end{pmatrix}, \tag{2.3}$$

where the matrix $\mathbb{R}_c$ is given by

$$\mathbb{R}_c = \begin{pmatrix} -\sin\lambda_c & \cos\lambda_c & 0 \\ -\sin\phi_c\cos\lambda_c & -\sin\phi_c\sin\lambda_c & \cos\phi_c \\ \cos\phi_c\cos\lambda_c & \cos\phi_c\sin\lambda_c & \sin\phi_c \end{pmatrix}.$$

Let ρ, p, T be the density, pressure, temperature of a parcel in terms of its coordinates xyz and $\mathrm{d}\mathbf{r}/\mathrm{d}t = \mathbf{v} = u\hat{\mathbf{x}} + v\hat{\mathbf{y}} + w\hat{\mathbf{z}}$. Then eq. (2.3) allows us to rewrite the governing equations (2.2a), (2.2b) as follows:

$$\begin{aligned} \frac{\mathrm{d}u}{\mathrm{d}t} + 2\Omega(w\cos\phi_c - v\sin\phi_c) &= -\frac{1}{\rho}\frac{\partial p}{\partial x} - g\frac{a^2}{r^3}x\,, \\ \frac{\mathrm{d}v}{\mathrm{d}t} + 2\Omega u\sin\phi_c &= -\frac{1}{\rho}\frac{\partial p}{\partial y} - g\frac{a^2}{r^3}y\,, \\ \frac{\mathrm{d}w}{\mathrm{d}t} - 2\Omega u\cos\phi_c &= -\frac{1}{\rho}\frac{\partial p}{\partial z} - g\frac{a^2}{r^3}(z+a)\,, \end{aligned} \tag{2.4a}$$

$$\frac{\mathrm{d}\log\rho}{\mathrm{d}t} + \frac{\partial u}{\partial x} + \frac{\partial v}{\partial y} + \frac{\partial w}{\partial z} = 0\,, \qquad p = \mathcal{R}T\rho\,, \qquad c_p\rho\frac{\mathrm{d}T}{\mathrm{d}t} = \frac{\mathrm{d}p}{\mathrm{d}t}\,, \tag{2.4b}$$

where $\mathrm{d}/\mathrm{d}t = \partial/\partial t + u(\partial/\partial x) + v(\partial/\partial y) + w(\partial/\partial z)$. If ρ_s, p_s, T_s are the density, pressure and temperature expressed in spherical coordinates $\lambda\phi r$ and u_s, v_s, w_s the longitudinal, latitudinal and radial velocity components, the transformation equations

$$X = r\cos\phi\cos\lambda\,, \qquad Y = r\cos\phi\sin\lambda\,, \qquad Z = r\sin\phi\,, \tag{2.5}$$

allow us to rewrite eqs. (2.2a), (2.2b) as follows:

$$\frac{\mathrm{d}u_s}{\mathrm{d}t} - \frac{u_s v_s}{r}\tan\phi + \frac{u_s w_s}{r} - 2\Omega v_s \sin\phi + 2\Omega w_s \cos\phi = -\frac{1}{\rho_s}\frac{1}{r\cos\phi}\frac{\partial p_s}{\partial\lambda}\,, \tag{2.6}$$

$$\frac{\mathrm{d}v_s}{\mathrm{d}t} + \frac{u_s^2}{r}\tan\phi + \frac{v_s w_s}{r} + 2\Omega u_s \sin\phi = -\frac{1}{\rho_s}\frac{1}{r}\frac{\partial p_s}{\partial\phi}\,,$$

$$\frac{\mathrm{d}w_s}{\mathrm{d}t} - \frac{u_s^2 + v_s^2}{r} - 2\Omega u_s \cos\phi = -\frac{1}{\rho_s}\frac{\partial p_s}{\partial r} - g\frac{a^2}{r^2}\,,$$

$$\frac{\mathrm{d}\log\rho_s}{\mathrm{d}t} + \frac{1}{r\cos\phi}\left[\frac{\partial u_s}{\partial\lambda} + \frac{\partial}{\partial\phi}\left(v_s\cos\phi\right)\right] + \frac{\partial w_s}{\partial r} + 2\frac{w_s}{r} = 0\,,$$

$$p_s = \mathcal{R}T_s\rho_s\,, \qquad c_p\rho_s\frac{\mathrm{d}T_s}{\mathrm{d}t} = \frac{\mathrm{d}p_s}{\mathrm{d}t}\,,$$

where $\dfrac{\mathrm{d}}{\mathrm{d}t} = \dfrac{\partial}{\partial t} + \dfrac{u_s}{r\cos\phi}\dfrac{\partial}{\partial\lambda} + \dfrac{v_s}{r}\dfrac{\partial}{\partial\phi} + w_s\dfrac{\partial}{\partial r}$.

3. – Approximate momentum equations

The momentum equations (2.4a) with respect to the tangent plane (x, y) will be referred to as the *exact equations* since they consider the exact gravity force (2.1) while the standard mesoscale literature use an approximation of these equations that omits the horizontal components of the gravity acceleration [2-12]. To get the last equations, consider the Taylor series

$$ga^2 r^{-3}x = -g\bar{x} + O(\bar{R}^2)\,,$$
$$ga^2 r^{-3}y = -g\bar{y} + O(\bar{R}^2)\,,$$
$$ga^2 r^{-3}(z+a) = -g + 2g\bar{z} + O(\bar{R}^2)\,,$$

where we use the dimensionless variables $\bar{x} = x/a$, $\bar{y} = y/a$, $\bar{z} = z/a$, $\bar{R} = r/a = \left[\bar{x}^2 + \bar{y}^2 + (1+\bar{z})^2\right]^{1/2}$. Hence we get the zeroth-order momentum equations

$$\frac{\mathrm{d}u^0}{\mathrm{d}t} + 2\Omega\left(w^0\cos\phi_c - v^0\sin\phi_c\right) = -\frac{1}{\rho^0}\frac{\partial p^0}{\partial x}\,, \tag{3.1}$$

$$\frac{\mathrm{d}v^0}{\mathrm{d}t} + 2\Omega u^0\sin\Omega_c = -\frac{1}{\rho^0}\frac{\partial p^0}{\partial y}\,,$$

$$\frac{\mathrm{d}w^0}{\mathrm{d}t} - 2\Omega u^0\cos\phi_c = -\frac{1}{\rho^0}\frac{\partial p^0}{\partial z} - g$$

and the complementary equations are

$$\frac{\mathrm{d}\log\rho^0}{\mathrm{d}t} + \frac{\partial u^0}{\partial x} + \frac{\partial v^0}{\partial y} + \frac{\partial w^0}{\partial z} = 0\,, \quad p^0 = \mathcal{R}T^0\rho^0\,, \quad c_p\rho^0\frac{\mathrm{d}T^0}{\mathrm{d}t} = \frac{\mathrm{d}p^0}{\mathrm{d}t}\,,$$

where the superscript "0" is used to distinguish the solutions of these equations from those of eqs. (2.4a), (2.4b). In a similar way we have the first-order equations

$$\begin{aligned} \frac{\mathrm{d}u^1}{\mathrm{d}t} + 2\Omega(w^1\cos\phi_c - v^1\sin\phi_c) &= -\frac{1}{\rho^1}\frac{\partial p^1}{\partial x} - g\bar{x}\,, \\ \frac{\mathrm{d}v^1}{\mathrm{d}t} + 2\Omega u^1\sin\phi_c &= -\frac{1}{\rho^1}\frac{\partial p^1}{\partial y} - g\bar{y}\,, \\ \frac{\mathrm{d}w^1}{\mathrm{d}t} - 2\Omega u^1\cos\phi_c &= -\frac{1}{\rho^1}\frac{\partial p^1}{\partial z} - g + 2g\bar{z} \end{aligned} \tag{3.2}$$

and

$$\frac{\mathrm{d}\log\rho^1}{\mathrm{d}t} + \frac{\partial u^1}{\partial x} + \frac{\partial v^1}{\partial y} + \frac{\partial w^1}{\partial z} = 0\,, \quad p^1 = \mathcal{R}T^1\rho^1\,, \quad c_p\rho^1\frac{\mathrm{d}T^1}{\mathrm{d}t} = \frac{\mathrm{d}p^1}{\mathrm{d}t}.$$

Some authors have pointed out that the momentum equations (3.1) are not well suited for practical applications [16, 1]. For instance, McVittie considers that the range of validity of eqs. (3.1) is very small but he did not provide an estimation of such a range. Other authors consider that if the horizontal scale L ($|x|, |y| \leq L$) is of order 10^3 km or smaller, the atmospheric flows can be located in the coordinate system xyz linked to the tangent plane normal to the gravity force [7]. Accordingly, eqs. (3.1) are used in several references [2-12] to theoretical analyses and computational mesoscale models use the same type of momentum equations in $xy\sigma_z$- or $xy\sigma_p$-coordinates (see, *e.g.*, [13-15]). However, some applications of these models to air-pollution studies have used horizontal domains

$$(x, y) \in \mathcal{D}(L) = [-L, L] \times [-L, L]$$

with $L \gtrsim 650$ km but the numerical results reported below suggest that zeroth-order equations like (3.1) are valid on a domain $\mathcal{D}(L)$ with $L \lesssim 100$ km.

In order to estimate the domain $\mathcal{D}(L)$ of validity of eqs. (3.1) and (3.2), we consider that the velocity field $\mathbf{v}$ is stationary, known, and satisfies the continuity equation and the pertinent boundary conditions. Then the isobars corresponding to the exact and approximate momentum equations are computed and their differences will be used to estimate the desired domains.

We consider the isobars on the plane $\mathcal{P}_\theta$ normal to the tangent plane (x, y) as fig. 2 shows. The isobars generated by the intersection of $\mathcal{P}_\theta$ with a pressure constant surface p_0,

$$p(x, y, z) = p_0, \tag{3.3a}$$

have the parametric equations

$$x = \xi\cos\theta\,, \qquad y = \xi\sin\theta\,, \qquad z = f(\xi)\,, \tag{3.3b}$$

where ξ and θ are the polar coordinates in the (x, y)-plane. From (3.3a), (3.3b) we get the isobar equation

$$\frac{\mathrm{d}f(\xi)}{\mathrm{d}\xi} = -\frac{\cos\theta\ \partial_x p + \sin\theta\ \partial_y p}{\partial_z p}\,, \tag{3.4}$$

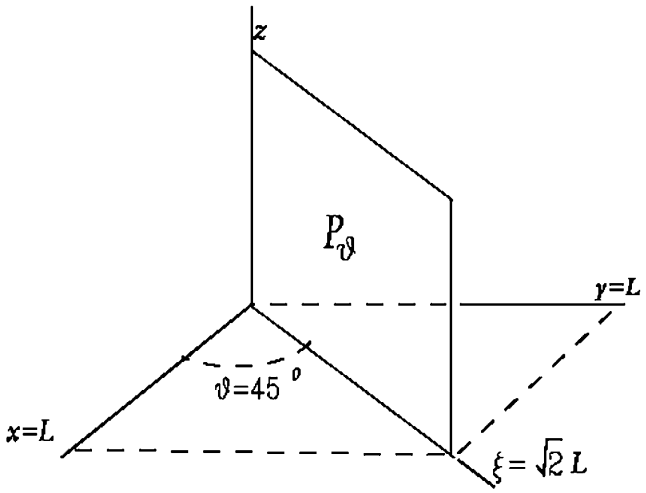

Fig. 2. – Sketch of the plane $\mathcal{P}_\theta$ with $\theta = 45°$.

where partial derivatives $\partial/\partial\tau$ are denoted by ∂_τ and $\partial_x p$, $\partial_y p$, $\partial_z p$ are obtained from the exact equations (2.4a). The solution of (3.4) with the boundary condition

$$f(\xi = 0) = z_0 \tag{3.5}$$

yields the isobar passing through $(\xi = 0, z_0)$. In a similar way the solution of equations

$$\begin{aligned} \frac{\mathrm{d}f^0(\xi)}{\mathrm{d}\xi} &= -\frac{\cos\theta\ \partial_x p^0 + \sin\theta\ \partial_y p^0}{\partial_z p^0}\,, \\ \frac{\mathrm{d}f^1(\xi)}{\mathrm{d}\xi} &= -\frac{\cos\theta\ \partial_x p^1 + \sin\theta\ \partial_y p^1}{\partial_z p^1} \end{aligned} \tag{3.6}$$

with a condition like (3.5) provides the isobars corresponding to the approximate equations (3.1) and (3.2). With this procedure we do not need to know the pressure fields in terms of x, y, z and the differences between f and f^0, f^1 yield an estimation of the reliability region $\mathcal{D}(L)$ of eqs. (3.1) and (3.2). The isobars on the plane $\mathcal{P}_\theta$ with $\theta = 45°$ are computed in order to obtain the largest difference between f and f^0, f^1 as ξ goes from 0 to $\sqrt{2}L$, which is the maximum ξ value for a given L. In this way we will estimate *upper bounds* $L^0_{\max}$ and $L^1_{\max}$ for the validity domains of the approximate equations (3.1) and (3.2).

There are three domains which illustrate the magnitude of the domains used in mesoscale modelation, namely, the domains $\mathcal{D}_a$, $\mathcal{D}_b$ with $L_a \sim 665$ km and $L_b \sim 882$ km were used in the study of regional transport of atmospheric pollutants [17, 22], and $\mathcal{D}_c$ with $L_c \sim 1665$ km is used in the operational meteorological analysis of México [23]. This latter domain provides the bound $\xi_{\max} = \sqrt{2}L = 2335$ km to define the range of ξ in figs. 3, 5, 6.

3˙1. *Hydrostatic and isothermic atmosphere.* – The simplest problem is a hydrostatic and isothermic atmosphere on the terrestrial sphere. It is easier to solve the equations

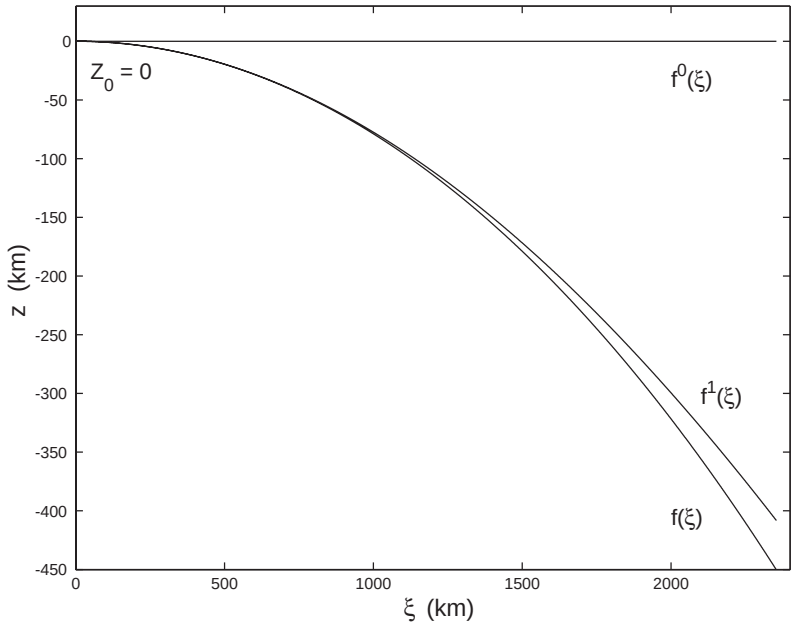

Fig. 3. – Isobars f, f^0, f^1 (eqs. (3.7)-(3.9)) on the plane $P_{\theta=45^\circ}$, which pass by the origin $(\xi = 0, z_0 = 0)$ of the xyz-system on the terrestrial sphere.

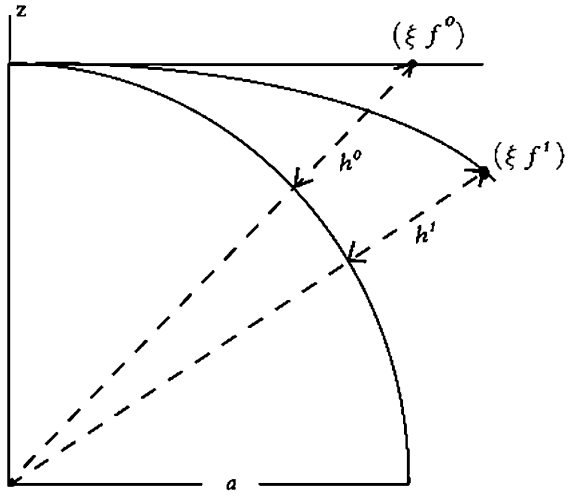

Fig. 4. – Sketch of the isobars f^0, f^1 of fig. 3 and their height h^0, h^1 with respect to the terrestrial sphere, which coincides with the exact isobar f.

in spherical coordinates. The continuity equation $\partial_t \rho_s = 0$ is satisfied by ρ_s independent of t and the horizontal momentum equations $\partial_\lambda p_s = 0$ and $\partial_\phi p_s = 0$ imply that p_s only depends on r. Hence, the pressure constant surfaces are spheres with radius r and center at the origin of the primary system XYZ. Thus the equation of the exact isobar $f(\xi)$ on $\mathcal{P}_\theta$ that satisfies (3.5) is

$$f(\xi) = -a + \sqrt{(z_0 + a)^2 - \xi^2}. \tag{3.7}$$

This result can be verified by solving (3.4), which becomes

$$\frac{\mathrm{d}f(\xi)}{\mathrm{d}\xi} = -\frac{\xi}{a + f(\xi)},$$

with the condition (3.5). From the zeroth-order equations (3.1), $\partial_x p^0 = \partial_y p^0 = 0$, $\partial_z p^0 = -\rho^0 g$, we get $\mathrm{d}f^0(\xi)/\mathrm{d}\xi = 0$ whose solution with (3.5) is

$$f^0(\xi) = z_0\,. \tag{3.8}$$

The first-order equations (3.2), $\partial_x p^1 = -\rho^1 g\bar{x}$, $\partial_y p^1 = -\rho^1 g\bar{y}$, $\partial_z p^1 = \rho^1 g(2\bar{z} - 1)$, yield

$$\frac{\mathrm{d}f^1(\xi)}{\mathrm{d}\xi} = \frac{\xi}{2f^1(\xi) - a}\,,$$

whose solution with condition (3.5) is

$$f^1(\xi) = \frac{1}{2}\left[a - \sqrt{a^2 + 2\xi^2 + 4z_0(z_0 - a)}\right]. \tag{3.9}$$

Figure 3 shows the graph of ξ *vs.* f, f^0, f^1 for $\xi \in [0, 2355\ \mathrm{km}]$ and $z_0 = 0$, we observe that f^0 moves away rapidly from the exact f as ξ increases, while f^1 exhibits an appreciable separation for $\xi \geq 10^3$ km.

The error of f^0 and f^1 can be shown with the graph of their height with respect to the terrestrial sphere. According to fig. 4 the height of a point $(\xi, f^0(\xi))$ on the isobar f^0 passing through $(\xi = 0, z_0 = 0)$ is

$$h^0(\xi) = -a + \sqrt{a^2 + \xi^2} \tag{3.10}$$

and for a point $(\xi, f^1(\xi))$ on the corresponding isobar f^1 we have

$$h^1(\xi) = -a + \sqrt{\xi^2 + [a + f^1(\xi)]^2}. \tag{3.11}$$

Figure 5 shows the graphs of ξ *vs.* h^0, h^1. We observe that if the pressure on the earth surface is $p_0 = 1013$ mb, the zeroth-order equations yield the same pressure value at the point $(\xi = 940, f^0(\xi))$ whose height on the earth surface is $h^0(\xi) \sim 600$ km, a wrong result and worse results are obtained as ξ tends to $\xi_{\max} = 2355$ km.

The functions h^0, h^1 defined by the isobars with $p_0 = 1013$ mb can be used to estimate upper bounds $L^0_{\max}$ and $L^1_{\max}$ for the validity domains of the approximate momentum equations. For instance, if we consider that $h_{\max}$ is the maximum height at which the

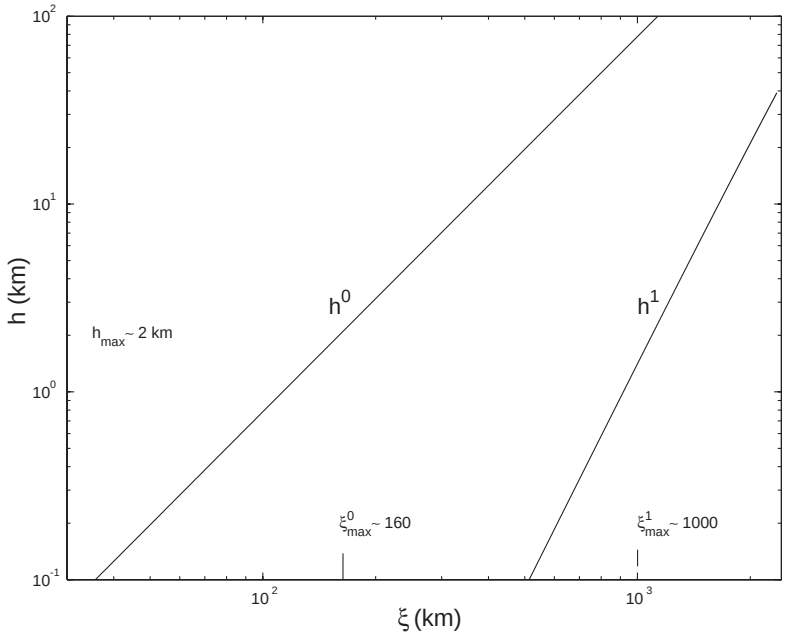

Fig. 5. – Graph of ξ *vs.* the height h^0, h^1 of the isobars f^0, f^1 of fig. 3.

pressure $p^0(\xi, z = f^0(\xi))$ is 1013 mb, then eq. (3.10) yields the corresponding $\xi^0_{\max}$ coordinate,

$$\xi^0_{\max} = \sqrt{(h_{\max} + a)^2 - a^2}, \tag{3.12a}$$

which provides the bound

$$L^0_{\max} = \xi^0_{\max}/\sqrt{2} \tag{3.12b}$$

for the reliability domain $\mathcal{D}(L^0_{\max})$ of the zeroth-order equations. It is clear that for any point (ξ, z_0) with $\xi < \xi^0_{\max}$ the error of numerical results from zeroth-order equations is lower than the error at $(\xi^0_{\max}, z_0)$. Let us consider

$$h_{\max} \sim 2 \text{ km},$$

then $\xi^0_{\max} \sim 160$ km and

$$L^0_{\max} \sim 113 \text{ km},$$

a result consistent with the small separation between f and f^0 in fig. 3 for $\xi \in [0, 100 \text{ km}]$. This yields the domain $\mathcal{D}(113 \text{ km})$ which is small with respect to the domain $\mathcal{D}_a(665 \text{ km})$ used in [17] where momentum equations of zeroth-order type in coordinates $xy\sigma_z$ were employed [15, 17].

Let us consider the reliability domain for first-order equations. Instead of computing $\xi^1_{\max}$ from eq. (3.11), it can be estimated from fig. 5 for a given $h_{\max}$. If $h_{\max} \sim 2$ km

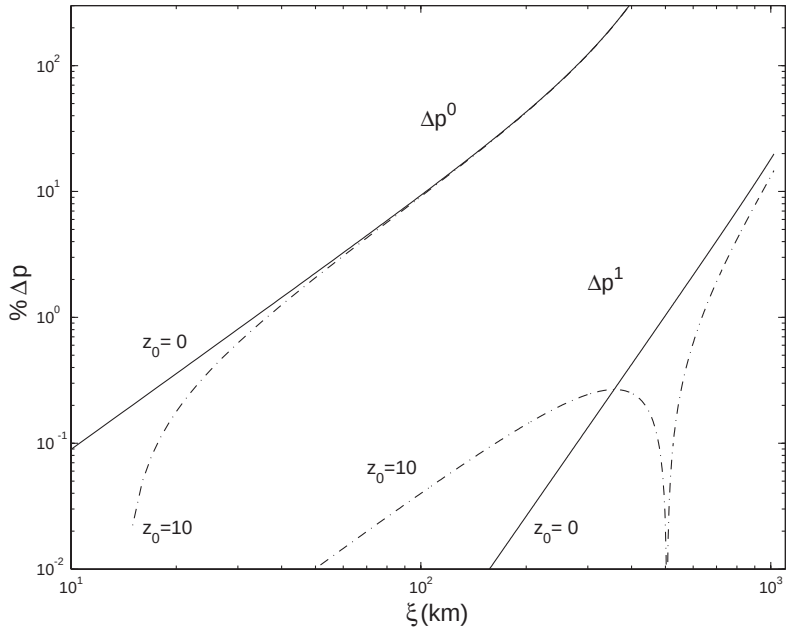

Fig. 6. – Graph of ξ *vs.* the relative error Δp^0, Δp^1 (3.16) of the pressure fields p^0 and p^1 on the terrestrial sphere ($z_0 = 0$) and the sphere with radius $r = 10$ km $+ a$, $a = 6378$ km.

we have $\xi^1_{\max} \sim 1000$ km and

$$L^1_{\max} \sim 700 \text{ km}.$$

This result is consistent with the small separation between f and f^1 in fig. 5 for $\xi \in [0, 1000 \text{ km}]$. The domain $\mathcal{D}(700)$ is similar to that D_a used in [17] and may be large enough for some applications of computational mesoscale models. This suggests the use of first-order momentum equations, which require a minimum modification of the zeroth-order equations used by some mesoscale models [14, 15].

The above results are independent of the explicit expressions of p^0, p^1, p in terms of x, y, z but if such expressions are known, we can compute the relative error of p^0, p^1 to estimate the reliability domain of the approximate momentum equations. Consider an isothermic and hydrostatic atmosphere with temperature T_0 and pressure p_0 on the terrestrial sphere. To compute p and ρ, it is easier to solve the equations in spherical coordinates (2.6), namely, $\partial p_s/\partial r = -\rho_s g a^2/r^2$ and $p_s = \mathcal{R}T_0\rho_s$ with $p_s(r = a) = p_0$. The solution

$$p_s(r) = p_0 e^{-ba(1-a/r)},$$

where $r = [x^2 + y^2 + (z + a)^2]^{1/2}$ and $b \equiv g/\mathcal{R}T_0$, yields $p(x, y, z) = p_s(r)$ which is the solution of the exact momentum equations with the boundary condition $p = p_0$ on the terrestrial sphere. In fact, the solution of eqs. (2.4a), (2.4b), or, equivalently,

$$\partial_x \ln p = -ba^2 x r^{-3}, \quad \partial_y \ln p = -ba^2 y r^{-3}, \quad \partial_z \ln p = -ba^2(z + a) r^{-3},$$

is $\ln p = ba^2/r + c$ and using $p\,|_{x=y=z=0} = p_0$ we get $p = p_0 e^{-ba(1-a/r)}$ which is the pressure field on the *whole* terrestrial sphere. This confirms that the governing equations (2.4a), (2.4b) in the xyz-system are equivalent to the equations in spherical coordinates (2.6) and, therefore, are valid on *any* domain $\mathcal{D}(L)$ indeed. Hence we get the pressure value on the isobar f that passes through the z-axis point $(\xi = 0, z = z_0)$, namely,

$$p(x = y = 0, z_0) = p_0 \exp[-bz_0/(1 + z_0/a)]\,. \tag{3.13}$$

The solution of zeroth-order equations (3.1) with $p^0(x = y = z = 0) = p_0$ is

$$p^0(z) = p_0 e^{-bz} \tag{3.14}$$

and for the first-order equations we have

$$p^1(\xi, z) = p_0 \exp\left[-\frac{b}{a}\left(\frac{1}{2}\xi^2 - z^2 + az\right)\right]. \tag{3.15}$$

Consider the relative error of p^0, p^1 on a sphere with radius $r = z_0 + a$ and center at the origin of the XYZ system, that is

$$\Delta p^i(\xi) = (p^i/p - 1)100 \qquad \text{with} \quad z = -a + \sqrt{(a + z_0)^2 - \xi^2} \tag{3.16}$$

and p is given by (3.13). The values $T_0 = 300\,\mathrm{K}$, $\mathcal{R} = 287$ J/kg K, $p_0 = 1013$ mb, $g = 9.8$ ms^{-2} and $a = 6378$ km yield $b = 0.11382$ km^{-1}. Figure 6 shows the graphs of ξ *vs.* Δp^0, Δp^1 on the earth surface ($z_0 = 0$) and the sphere with radius $r = z_0 + a$ and $z_0 = 10$ km. We observe that Δp^0 is less than 20% for $\xi \le \xi^0_{\max} \sim 160$ km and increases rapidly from 20 to 300% as ξ goes from $\xi^0_{\max}$ to 400 km. In contrast, the error Δp^1 is smaller than 20% for $\xi \le \xi^1_{\max} \sim 1000$ km. This confirms that $\xi^0_{\max} \sim 160$ km, $\xi^1_{\max} \sim 1000$ km provide upper bounds $L^0_{\max} \sim 113$ km, $L^1_{\max} \sim 700$ km for the reliability domains $\mathcal{D}(L^0_{\max})$, $\mathcal{D}(L^1_{\max})$ of the approximate equations (3.1) and (3.2).

3˙2. *Bidimensional steady motion.* – Consider the flow on $\mathcal{P}_\theta$ obtained from the flow around a circular cylinder,

$$\mathbf{v}\,(\xi, z) = U\left(\bar{\xi}, \bar{z}\right)\widehat{\boldsymbol{\xi}} + W\left(\bar{\xi}, \bar{z}\right)\widehat{\mathbf{z}}$$

with

$$U = U_0(1 + \overline{R}^{-2} - 2\overline{\xi}^2\overline{R}^{-4})\,, \qquad W = -2U_0\overline{\xi}\,(1 + \overline{z})\,\overline{R}^{-4}\,. \tag{3.17}$$

Using $\overline{\xi}^2 = \overline{x}^2 + \overline{y}^2$ and $\widehat{\boldsymbol{\xi}} = \cos\theta\hat{\mathbf{x}} + \sin\theta\hat{\mathbf{y}}$ we get the velocity field $\mathbf{v} = u\hat{\mathbf{x}} + v\hat{\mathbf{y}} + w\hat{\mathbf{z}}$,

$$u = U\left(\bar{\xi}, \bar{z}\right)\cos\theta\,, \qquad v = U\left(\bar{\xi}, \bar{z}\right)\sin\theta\,, \qquad w = W\left(\bar{\xi}, \bar{z}\right), \tag{3.18}$$

which satisfies the continuity equation $\boldsymbol{\nabla} \cdot \mathbf{v} = 0$ and the correct boundary condition $\mathbf{v} \cdot \mathbf{n}\,|_{z=z_e(x,y)} = 0$ where $\mathbf{n}$ is normal to the terrestrial sphere which has the equation

$$z_e\,(x, y) = -a + \sqrt{a^2 - x^2 - y^2}.$$

By replacing (3.18) in eqs. (3.4) and (3.6) we get the isobar equations

$$
\begin{aligned}
\frac{\mathrm{d}f\,(\xi)}{\mathrm{d}\xi} &= -\frac{a^{-1}\mathbb{M}U + 2\Omega W\cos\phi_c\cos\theta + \bar{\xi}g/\ \bar{R}^3}{a^{-1}\mathbb{M}W - 2\Omega U\cos\theta\cos\phi_c + g\ (1+\bar{z})\ /\ \bar{R}^3}\,, \\
\frac{\mathrm{d}f^0\,(\xi)}{\mathrm{d}\xi} &= -\frac{a^{-1}\mathbb{M}U + 2\Omega W\cos\phi_c\cos\theta}{a^{-1}\mathbb{M}W - 2\Omega U\cos\theta\cos\phi_c + g}\,, \\
\frac{\mathrm{d}f^1\,(\xi)}{\mathrm{d}\xi} &= -\frac{a^{-1}\mathbb{M}U + 2\Omega W\cos\phi_c\cos\theta + \bar{\xi}g}{a^{-1}\mathbb{M}W - 2\Omega U\cos\theta\cos\phi_c + g\ (1-2\bar{z})}\,,
\end{aligned}
\tag{3.19}
$$

where $\mathbb{M} = U\partial_{\bar{\xi}} + W\partial_{\bar{z}}$ and whose solution with the boundary condition (3.5) yields the isobars that pass through $(\xi = 0, z_0)$. The graph of ξ *vs.* f^0, f^1, f for $\xi \in [0, 1000\ \mathrm{km}]$ and $U_0 = 10\ \mathrm{ms}^{-1}$ has no appreciable difference with fig. 3. Thus, if we use the isobar heights h^0 and h^1 to estimate the validity region of the approximate momentum equations, such regions are equal to those estimated for the hydrostatic case. In particular, if $h_{\max} \sim 2$ km is the largest height of the isobars f^0, f^1 corresponding to the earth surface pressure p_0, then $\mathcal{D}(L^0_{\max}) \lesssim 200 \times 200\ \mathrm{km}^2$ and $\mathcal{D}(L^1_{\max}) \lesssim 1400 \times 1400\ \mathrm{km}^2$.

The similarity between the isobars f, f^0, f^1 from eqs. (3.19) and those for the hydrostatic case is expected because the factors a^{-1} and Ω reduce significantly the contribution of the velocity components with respect to g. This argument can be extrapolated to any large-scale velocity field $\mathbf{v}$ with u, $v \sim 10\ \mathrm{m\ s}^{-1}$ and $w \sim 10^{-2}\ \mathrm{m\ s}^{-1}$, so that in general we can expect that the differences between f, f^0, f^1 will be similar to those observed in fig. 3 and, therefore, $\mathcal{D}(L^0_{\max})$ and $\mathcal{D}(L^1_{\max})$ will be as above.

4. – Equations from map projections

To analyze the role of map projections, we begin with a formal definition of $x_p y_p H_p$ which will be called projection coordinates. Let $x_p y_p$ be a Cartesian coordinate system on a projection plane $\mathcal{P}$ which is normal to the H_p-axis. The projection of a point (λ, ϕ) on the terrestrial sphere is the point (x_p, y_p) given by a pair of projections equations

$$
x_p = x_p(\lambda, \phi)\,, \qquad\qquad y_p = y_p(\lambda, \phi). \tag{4.1a}
$$

Usually, the center (λ_c, ϕ_c) of the horizontal domain $\mathcal{D}$ on the tangent plane xy is projected on the origin of the $x_p y_p$-system,

$$
x_p(\lambda_c, \phi_c) = y_p(\lambda_c, \phi_c) = 0, \tag{4.1b}
$$

and the eastward parallel circle and the northward meridian on (λ_c, ϕ_c) are projected on the positive x_p- and y_p-axes, respectively. If a point in physical space has spherical coordinates (λ, ϕ, r), its coordinates x_p, y_p are given by (4.1a) and H_p is defined by

$$
H_p = r - a. \tag{4.1c}
$$

Thus we have four equivalent sets of coordinates to define the position of a parcel, namely, (x, y, z), (X, Y, Z) and (λ, ϕ, r) which have a simple geometrical interpretation in physical space while (x_p, y_p, H_p) are coordinates in an abstract space. If we assume that the

projection is conformal, $x_p y_p H_p$ are orthogonal curvilinear coordinates and the governing equations in such coordinates are obtained from the equations in spherical coordinates [18]. If ρ_p, p_p, T_p are the density, pressure and temperature in projection coordinates and $u_p v_p w_p$ are the corresponding velocity components, the governing equations are

$$
\begin{aligned}
(4.2)\qquad & \frac{\mathrm{d}}{\mathrm{d}t}\begin{pmatrix} u_p \\ v_p \end{pmatrix} + \left(r^{-1}u_p \tan\phi + f\right)\begin{pmatrix} -v_p \\ u_p \end{pmatrix} + r^{-1}w_p \begin{pmatrix} u_p \\ v_p \end{pmatrix} + \\
& + \mathbb{T}\left[h_\lambda^{-1}u_p\left(\partial_\lambda \mathbb{T}^t\right) + h_\phi^{-1}v_p\left(\partial_\phi \mathbb{T}^t\right)\right]\begin{pmatrix} u_p \\ v_p \end{pmatrix} + \\
& + \mathbb{T}\begin{pmatrix} 2\Omega w_p \cos\phi \\ 0 \end{pmatrix} = \; -\rho_p^{-1}\begin{pmatrix} h_x^{-1}\partial_{x_p} p_p \\ h_y^{-1}\partial_{y_p} p_p \end{pmatrix},
\end{aligned}
$$

$$
\frac{\mathrm{d}w_p}{\mathrm{d}t} - \frac{u_p^2 + v_p^2}{r} - 2\Omega u_s \cos\phi = -\frac{1}{\rho_p}\frac{\partial p_p}{\partial H_p} - \frac{ga^2}{r^2},
$$

$$
\frac{\mathrm{d}\rho_p}{\mathrm{d}t} + \rho_p \frac{1}{h_x h_y}\left[\frac{\partial}{\partial x_p}\left(h_y u_p\right) + \frac{\partial}{\partial y_p}\left(h_x v_p\right) + \frac{\partial}{\partial z_p}\left(h_x h_y w_p\right)\right] = 0
$$

and $p_p = \mathcal{R}T_p\rho_p$, where $f = 2\Omega\sin\phi$, the matrix $\mathbb{T}$ and the metric factors h_x, h_y depend on the projection in question (see appendix) and

$$
\frac{\mathrm{d}}{\mathrm{d}t} = \frac{\partial}{\partial t} + \frac{u_p}{h_x}\frac{\partial}{\partial x_p} + \frac{v_p}{h_y}\frac{\partial}{\partial y_p} + w_p\frac{\partial}{\partial H_p}.
$$

The solution of these equations with the pertinent boundary and initial conditions generates the meteorological fields in the $x_p y_p H_p$ space but in order to analyze such fields in physical space we have to apply the following coordinate transformations to obtain the fields in Cartesian x, y, z or spherical λ, ϕ, r coordinates. From (4.1a)-(4.1c) we get λ, ϕ, r in terms of x_p, y_p, H_p,

$$
(4.3)\qquad \lambda = \lambda(x_p, y_p), \qquad \phi = \phi(x_p, y_p) \qquad r = H_p + a.
$$

From (2.3) and (2.5) we obtain x, y, z in terms of λ, ϕ, r and combining this result with (4.3) the relation between x, y, z and x_p, y_p, H_p follows

$$
(4.4)\qquad \begin{pmatrix} x \\ y \\ z + a \end{pmatrix} = \mathbb{R}_c \begin{pmatrix} (H_p + a)\cos\phi(x_p, y_p)\cos\lambda(x_p, y_p) \\ (H_p + a)\cos\phi(x_p, y_p)\sin\lambda(x_p, y_p) \\ (H_p + a)\sin\phi(x_p, y_p) \end{pmatrix}.
$$

This shows that xyz and $x_p y_p H_p$ are different coordinate systems. However, the references [6,18-21] that solve map-projection equations like (4.2) do not report or suggest the use of the coordinate transformations (4.3) or (4.4) to recover the meteorological fields from (4.2) in xyz- or $\lambda\phi r$-coordinates. Instead, the approximation

$$
(4.5)\qquad x_p \sim x, \qquad y_p \sim y, \qquad H_p \sim z,
$$

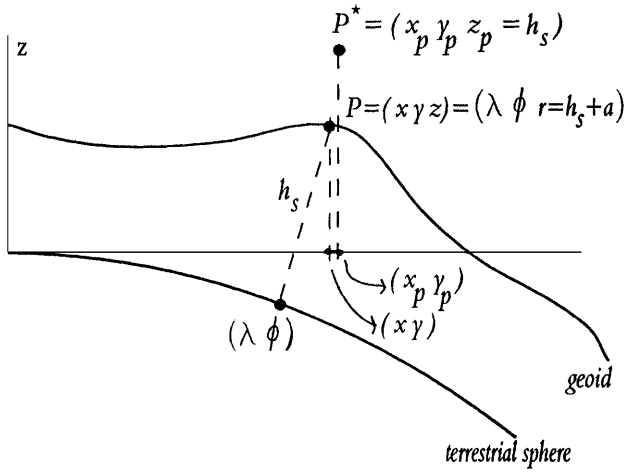

Fig. 7. – Sketch of a point P on the geoid and their coordinates xyz, $\lambda, \phi, r = h_s + a$, and $x_p, y_p, H_p = h_s$.

is used to work on the Cartesian coordinate system xy with the expectation that the map projection considers the spherical shape of the earth [6]. In fact, the usual horizontal coordinate system in mesoscale modeling is a Cartesian system xy [2-13] but some models attempt to consider the earth sphericity using map projections to define the topography [14, 15] and other models define both topography and governing equations like (4.2) with map projections [18-21]. Let us see more carefully this approach.

Although the standard terrain elevation data are referred to an ellipsoid we can consider that the data are known with respect to a spherical earth model defined properly from the ellipsoidal model [24]. Let $h_s(\lambda, \phi)$ denote the terrain elevation on the point (λ, ϕ) of the terrestrial sphere, then the set of points with spherical coordinates $(\lambda, \phi, r = h_s + a)$ define the true earth surface (which is called *geoid*) as fig. 7 shows. In practice the geoid is known only on a discrete set of points $(\lambda_k, \phi_k, r_k = h_{sk} + a)$, $k = 1, .., N$.

It is a common practice in mesoscale modeling, to define the topography from a data set $\{\lambda_k, \phi_k, h_{sk}\}$, computing a point (x_{pk}, y_{pk}) with a map projection (4.1a) and consider that the terrain elevation on (x_{pk}, y_{pk}) is $h_s(\lambda_k, \phi_k)$ since "map projections generate a minimum distortion of the earth surface". Of course, (x_{pk}, y_{pk}) is on the projection plane $\mathcal{P}$ in an abstract space $x_p y_p H_p$, but if the terrain height on the domain center (λ_c, ϕ_c) is *defined* as the datum $h_s(\lambda_c, \phi_c)$, the plane $\mathcal{P}$ can be identified as the plane $\mathcal{T}$ tangent to the earth at (λ_c, ϕ_c) (see [24] for details). Additionally, if the scale of the xy- and $x_p y_p$-systems is the same, then every point (x_p, y_p) defines a point in the xy-system. According to the definition of projection coordinates, it is clear that a point $P = \{\lambda, \phi, h_s\}$ on the geoid has projection coordinates $x_p, y_p, H_p = h_s$, spherical coordinates $\lambda, \phi, r = h_s + a$ and the *unique* and *correct* coordinates x, y, z of P are given by (4.4). If the projection coordinates (x_p, y_p, H_p) of P are seen as the coordinates of a point in physical space rather than in the space $x_p y_p H_p$, then such coordinates define the localization of point P^* different to P. This is clearly illustrated by (4.4) and fig. 7 which show that in

general we have

$$x \neq x_p\,, \qquad y \neq y_p\,, \qquad z \neq H_p\,.$$

Since map projections generate a minimum distortion of the terrestrial sphere, the horizontal coordinates are very similar over a wide range,

$$x \sim x_p\,, \qquad y \sim y_p.$$

For instance, figs. 4, 5 of ref. [24] show that the relative error $|y - y_p|\,/y$ is very small for $y \in [0, 1665\text{km}]$ and several map projections. Apparently this result justifies the use of the approximation (4.5) but the problem lies in the vertical coordinate. If (x_p, y_p) is close to the origin $(x = 0, y = 0) = (\lambda_c, \phi_c)$ the difference $|z - H_p|$ is small but it increases rapidly as x_p or y_p do. For example, the correct xyz-coordinates of the point with projection coordinates $x_p = 0$, $y_p = 650$ km, $H_p = 0$ are $x = 0$, $y \sim 650 \pm 8$ km, $z \sim -33$ km. Some of the most accurate terrain data available in the world wide web have the uncertainty $\Delta h_s = \pm 30$ m [25] and in ref. [24] it was shown that the approximation $H_p \sim z$ is consistent with this uncertainty on a horizontal domain

$$\mathcal{D}_h \sim 60 \times 60 \text{ km}^2 \tag{4.6}$$

which is very small with respect to the domains $\mathcal{D}_a$, $\mathcal{D}_b$, $\mathcal{D}_c$ used in [17, 22, 23].

In order to simplify the lower boundary conditions, most mesoscale models use governing equations with horizontal xy-coordinates and a vertical coordinate like

$$\sigma_z = z_{\max} \frac{z - z_h(x, y)}{z_{\max} - z_h(x, y)}\,,$$

where $z_h(x, y)$ is the correct terrain elevation on the point (x, y) in the tangent plane $\mathcal{T}$ and $z_{\max}$ is the height of the model domain [13]. If the approximation (4.5) is used, (x, y) is replaced by (x_p, y_p) and $z_h(x, y)$ by the terrain elevation $z_{hp}(x_p, y_p)$ from the geoid datum h_s,

$$z_{hp}(x_p, y_p) \equiv h_s[\lambda(x_p, y_p), \phi(x_p, y_p)] \tag{4.7}$$

which has an error $|z_{hp}(x_p, y_p) - z_h(x_p, y_p)|$ between 33 and 200 km for $(x_p, y_p) \in \mathcal{D}_c \setminus \mathcal{D}_a$ [24]. This leads to the approximate vertical coordinate

$$\sigma_{zp} = z_{\max} \frac{z - z_{hp}(x_p, y_p)}{z_{\max} - z_{hp}(x_p, y_p)}.$$

Following the standard literature, *zeroth-order* momentum equations were used in ref. [24] to analyze the effect of using a map-projection topography. According to the results of sect. **3** the correct analysis has to use the exact momentum equations (2.4). If this is done with the terrain elevation $h_s(\lambda, \phi) \equiv 0$, one obtains velocity fields $\mathbf{v}$ and $\mathbf{v}^0$ similar to those of ref. [24], which exhibit significant differences on a domain like $\mathcal{D}_a$, $\mathcal{D}_b$, $\mathcal{D}_c$, and the additional result that the difference between the exact isobar f and the approximate f^0 is similar to that observed in fig. 3. Thus, if the topography is defined via map projections (eq. (4.7)) and the approximation (4.5) is valid on the domain $\mathcal{D}_h$ (4.6), we

can say that the zeroth-order equations (3.1) in $xy\sigma_{zp}$-coordinates are valid on a domain $\mathcal{D}$ smaller than or equal to $\mathcal{D}_h$ (4.6) while the same equations in $xy\sigma_z$-coordinates with the correct topography $z_h(x,y)$ are valid on $\mathcal{D} \lesssim 200 \times 200$ km^2 (sect. **3**).

If the approximation (4.5) is used to solve the map-projection equations (4.2), we replace $x_p y_p H_p$ by xyz in (4.2) to obtain the equations

$$
\begin{aligned}
(4.8) \qquad & \frac{\mathrm{d}}{\mathrm{d}t}\begin{pmatrix} u_p^* \\ v_p^* \end{pmatrix} + \left(r^{-1}u_p^* \tan\phi + f\right)\begin{pmatrix} -v_p^* \\ u_p^* \end{pmatrix} + r^{-1}w_p^*\begin{pmatrix} u_p^* \\ v_p^* \end{pmatrix} + \\
& + \mathbb{T}\left[h_\lambda^{-1}u_p^*\left(\partial_\lambda \mathbb{T}^t\right) + h_\phi^{-1}v_p^*\left(\partial_\phi \mathbb{T}^t\right)\right]\begin{pmatrix} u_p^* \\ v_p^* \end{pmatrix} + \\
& + \mathbb{T}\begin{pmatrix} 2\Omega w_p^* \cos\phi \\ 0 \end{pmatrix} = -\rho_p^{*-1}\begin{pmatrix} h_x^{-1}\partial_x p_p^* \\ h_y^{-1}\partial_y p_p^* \end{pmatrix},
\end{aligned}
$$

$$
\frac{\mathrm{d}w_p^*}{\mathrm{d}t} - \frac{u_p^{*2} + v_p^{*2}}{r} - 2\Omega u_s^* \cos\phi = -\frac{1}{\rho_p^*}\frac{\partial p_p^*}{\partial z} - \frac{ga^2}{r^2},
$$

$$
\frac{\mathrm{d}\log\rho_p^*}{\mathrm{d}t} + \frac{1}{h_x h_y}\left[\frac{\partial}{\partial x}\left(h_y u_p^*\right) + \frac{\partial}{\partial y}\left(h_x v_p^*\right) + \frac{\partial}{\partial z}\left(h_x h_y w_p^*\right)\right] = 0
$$

and $p_p^* = \mathcal{R}T_p^*\rho_p^*$ with

$$
\frac{\mathrm{d}}{\mathrm{d}t} = \frac{\partial}{\partial t} + \frac{u_p^*}{h_x}\frac{\partial}{\partial x} + \frac{v_p^*}{h_y}\frac{\partial}{\partial y} + w_p^*\frac{\partial}{\partial z},
$$

where the superscript "*" is used to distinguish the solution of these equations from that of the correct equations (4.2) in the $x_p y_p H_p$ space. We observe that the horizontal momentum equations have no gravity-force term and therefore such equations are similar to the zeroth-order equations (3.1), a conclusion verified by the solution for an isothermic and hydrostatic atmosphere. In this case the equations

$$
\frac{\partial\rho_p^*}{\partial t} = \frac{\partial p_p^*}{\partial x} = \frac{\partial p_p^*}{\partial y} = 0, \qquad \frac{\partial p_p^*}{\partial z} = -\frac{ga^2}{(z+a)^2}\rho_p^*
$$

with $p_p^* = p_0$ (1013 mb) at $x = y = z = 0$ yield $p_p^* = p_0 e^{-baz/(z+a)}$ which is essentially the pressure $p^0(z)$ (3.14) from the zeroth-order equations (3.1) if we consider $|z| \ll a$. Thus we can say that the map-projection equations (4.8) are valid on $\mathcal{D}^0 \sim 200 \times 200$ km^2, and if these equations are rewritten in coordinates $xy\sigma_{zp}$ the reliability domain is $\mathcal{D}_h$ (4.6).

5. – Conclusions

There has been an important effort to develope computational mesoscale models which use the Cartesian coordinate system xyz, where z is replaced by a σ-type coordinate, and some of which use the momentum equation (1.3) [13]. Although eq. (1.3) is suitable for theoretical analysis of small-scale processes [2-12], it may not be well suited for the numerical mesoscale modeling of regional atmospheric flows. In agreement with other authors [1, 16], the results of subsect. **3**˙1 suggest that eq. (3.1) is valid on a horizontal

domain $\mathcal{D}(L^0_{\max}) \lesssim 200\times200$ km^2. Of course, the examples of sects. **3**, **4** ignore important factors controlling a real flow such as the stratification and, mainly, the time evolution which can generate important qualitative differences between the flows from eqs. (1.3) and (1.4) because of their nonlinearity. However, the numerical modeling of some mesoprocesses requires the use of a large domain $\mathcal{D}(L)$ i) to include the influence of propagating synoptic disturbances on the regional weather and ii) to reduce the error from the lateral boundary conditions inherent to limited-area modeling [10, 13]. In principle, this conflict can be solved with the use of the exact momentum equation (1.4), which is valid on any domain $\mathcal{D}(L)$, the correct initial and boundary conditions, the complementary conservation equations and the equation of state. In practice, $\mathcal{D}(L)$ will be limited by i) the available data to define the initial and boundary conditions and ii) the computational resources. For example, if $L = 500$ km and the height of the troposphere on the terrestrial sphere is $H = 18$ km we have to use a tridimensional model region with a height $H_M = |z|_{\max} + H \sim 57.3$ km, where

$$|z|_{\max} = \left|-a + \sqrt{a^2 - 2L^2}\right| \tag{5.1}$$

and $a = 6378$ km, which increases significantly the computational cost and probably the data from global prediction models are insufficient to define initial conditions.

If xyz ($\widehat{\mathbf{x}}\widehat{\mathbf{y}}\widehat{\mathbf{z}}$) are denoted by $x^1x^2x^3$ ($\widehat{\mathbf{x}}_1\widehat{\mathbf{x}}_2\widehat{\mathbf{x}}_3$), respectively, and we set

$$\tilde{x}^1 = x^1\,, \qquad \tilde{x}^2 = x^2\,, \qquad \tilde{x}^3 = \tilde{x}^3(x^1, x^2, x^3, t)\,, \tag{5.2}$$

the contravariant form of the gravitational acceleration (1.2) is

$$\mathbf{g} = g^j\hat{\mathbf{x}}_j = g^j\frac{\partial\tilde{x}^i}{\partial x^j}\boldsymbol{\tau}_i\,, \tag{5.3}$$

where

$$g^i = -ga^2\tilde{x}^i r^{-3} \ \text{ for } i = 1, 2, \qquad g^3 = -ga^2(z+a)r^{-3} \tag{5.4}$$

and $\boldsymbol{\tau}_i$ are the covariant vectors from the $\tilde{x}^j$'s. Hence, the contravariant form of the momentum equation (1.4) is

$$\frac{\partial\tilde{u}^i}{\partial t} = -\tilde{u}^j\tilde{u}^i_{,j} - \tilde{G}^{ij}\theta\frac{\partial\pi}{\partial\tilde{x}^j} + g^j\frac{\partial\tilde{x}^i}{\partial x^j} - 2\varepsilon^{ijl}\Omega_j\tilde{u}_l, \tag{5.5}$$

where frictional forces are neglected, instead of the contravariant form of the zeroth-order equation (1.3),

$$\frac{\partial\tilde{u}^i}{\partial t} = -\tilde{u}^j\tilde{u}^i_{,j} - \tilde{G}^{ij}\theta\frac{\partial\pi}{\partial\tilde{x}^j} - \frac{\partial\tilde{x}^i}{\partial x^3}g - 2\varepsilon^{ijl}\Omega_j\tilde{u}_l \tag{5.6}$$

[5, p. 110]. The practical limitations discussed above impose the use of a domain $\mathcal{D}(L)$ with $L \le 500$ km which is smaller than the bound $L^1_{\max} \lesssim 700$ km of the reliability domain of the first-order equations (3.2). Thus, we can use the linear approximation

$$g^1 \sim -gx/a\,, \qquad g^2 \sim -gy/a\,, \qquad g^3 \sim -g(1 - 2z/a) \tag{5.7}$$

in eq. (5.5). If $L = 500$ km we have $|z|_{\max} = 39.3$ km and hence $|2z/a| \leq 0.01$ so that the term $2z/a$ can be neglected. It has been pointed out that the variations of $\mathbf{g}$ due to height above the ground of location on the earth surface should be considered (see, *e.g.*, [5, p.16], [1, p. 225]). The reliability of the first-order equations (3.2) shows that the horizontal variation of $\mathbf{g}$ is more important than the vertical one in $\widehat{\mathbf{z}}$. In fact, if we use $\mathbf{g} \sim -ga^2(z+a)^{-2}\widehat{\mathbf{z}}$ in $-\vec{\nabla}p = \rho\mathbf{g}$ the pressure field $p \sim p_0 \exp[-baz/(z+a)]$ is similar to p^0 (3.14) while the approximation $\mathbf{g} \sim -g(x\hat{\mathbf{x}}+y\hat{\mathbf{y}}+a\hat{\mathbf{z}})/a$ yields $p \sim p_0 \exp[-\frac{b}{a}(\frac{1}{2}\xi^2+az)]$ which is basically p^1 (3.15).

The horizontal momentum equations reported in some references (see, *e.g.*, [17, eqs. (3,4)], [26]) have terms with g but it does not come from the use of the correct gravity acceleration $\mathbf{g}$ (1.2). For instance, from the *zeroth-order* equation (5.6), $\sigma_z = s(z - z_G)/(s - z_G)$, the hydrostatic relation and the chain rule Pielke [5, eq. (6-56)] obtains

$$\frac{\partial \tilde{u}^1}{\partial t} = -\tilde{u}^j \frac{\partial \tilde{u}^1}{\partial \tilde{x}^j} - \overline{\tilde{u}^j \frac{\partial \tilde{u}^1}{\partial \tilde{x}^j}} - \theta \frac{\partial \pi}{\partial \tilde{x}^1} + g\frac{\sigma - s}{s}\frac{\partial z_G}{\partial x} - \hat{f}u^3 + fu^2\,,$$

where the terms with g^1, g^2 or their linear approximation (5.7) are absent.

The use of projection coordinates $x_p y_p H_p$ in numerical modeling is correct when the initial and boundary conditions are obtained from real data in coordinates xyz or $\lambda\phi r$ via the inverse of the transformation equations (4.3), (4.4), but if $x_p y_p H_p$ are taken as approximations of xyz, as occurs with the definition of topography [24], the resulting momentum equations are basically zeroth-order momentum equations and hence their range of validity is very small. A similar problem may occur with the use of the curvilinear coordinates

$$x_s = (\lambda - \lambda_c)a\cos\phi_c\,, \qquad y_s = (\phi - \phi_c)a\,, \qquad z_s = r - a\,.$$

Let L, D be the horizontal and vertical scales of a flow on the terrestrial sphere. Some references [7, 27-29] use the coordinates $x_s y_s z_s$ to rewrite the governing equations in spherical coordinates in the expectation that for small L/a and D/a they will be the Cartesian coordinates of the β-plane approximation [27]. If $x_s y_s z_s$ are replaced by xyz, the resulting equations are approximations of the exact ones in xyz-coordinates, as occurs with eqs. (4.8). Of course, the equations in coordinates $x_s y_s z_s$ allow the study of dynamical effects from the latitudinal variation of the Coriolis force, for example, but one should be careful in consider such coordinates as xyz.

* * *

The author wishes to thank the referee for his comments, R. Maria Velasco and E. Caetano for the revision of the manuscript and Ma. Trinidad N. for her invaluable support.

Appendix

Let $\mathbf{R} = X\widehat{\mathbf{X}} + Y\widehat{\mathbf{Y}} + Z\widehat{\mathbf{Z}}$ be the position vector of an air parcel where X, Y, Z are functions of x_p, y_p, H_p. Hence we get the vectors

$$\mathbf{x}_p = \partial_{x_p}\mathbf{R}\,, \qquad \mathbf{y}_p = \partial_{y_p}\mathbf{R}\,, \qquad \mathbf{H}_p = \partial_{H_p}\mathbf{R}$$

with magnitudes $h_x \equiv \|\mathbf{x}_p\|$, $h_y \equiv \|\mathbf{y}_p\|$, $h_z \equiv \|\mathbf{H}_p\| = 1$ and

$$\widehat{\mathbf{x}}_p = \mathbf{x}_p/h_x\,, \qquad \widehat{\mathbf{y}}_p = \mathbf{y}_p/h_y\,, \qquad \widehat{\mathbf{H}}_p = \mathbf{H}_p\,.$$

For $\mathbf{R} = X\widehat{\mathbf{X}} + Y\widehat{\mathbf{Y}} + Z\widehat{\mathbf{Z}}$ in spherical coordinates we have

$$\boldsymbol{\lambda} = \partial_\lambda\mathbf{R}\,, \qquad \boldsymbol{\phi} = \partial_\phi\mathbf{R}\,, \qquad \mathbf{r} = \partial_r\mathbf{R}$$

with $h_\lambda = \|\boldsymbol{\lambda}\| = r\cos\phi$, $h_\phi = \|\boldsymbol{\phi}\| = r$, $h_r = \|\mathbf{r}\| = 1$ and

$$\widehat{\boldsymbol{\lambda}} = \boldsymbol{\lambda}\,/h_\lambda\,, \qquad \widehat{\boldsymbol{\phi}} = \boldsymbol{\phi}\,/h_\phi\,, \qquad \widehat{\mathbf{r}} = \mathbf{r}\,.$$

Considering that the projection (4.1a) is conformal and $\widehat{\mathbf{x}}_p \times \widehat{\mathbf{y}}_p = \widehat{\mathbf{H}}_p$ we find the relation

$$\begin{pmatrix} \widehat{\mathbf{x}}_p \\ \widehat{\mathbf{y}}_p \end{pmatrix} = \mathbb{T}\,(\lambda,\phi) \begin{pmatrix} \widehat{\boldsymbol{\lambda}} \\ \widehat{\boldsymbol{\phi}} \end{pmatrix},$$

where

$$\mathbb{T}\,(\lambda,\phi) = \begin{pmatrix} T_1 & T_2 \\ -T_2 & T_1 \end{pmatrix} \equiv \frac{1}{\Delta} \begin{pmatrix} (\partial_\phi y_p)\,h_\lambda h_x^{-1} & -(\partial_\lambda y_p)\,h_\phi h_x^{-1} \\ -(\partial_\phi x_p)\,h_\lambda h_y^{-1} & (\partial_\lambda x_p)\,h_\phi h_y^{-1} \end{pmatrix},$$

$$h_x = \Delta^{-1}\sqrt{\left[(\partial_\phi y_p)\,h_\lambda\right]^2 + \left[(\partial_\lambda y_p)\,h_\phi\right]^2}\,,$$

$$h_y = \Delta^{-1}\sqrt{\left[(\partial_\phi x_p)\,h_\lambda\right]^2 + \left[(\partial_\lambda x_p)\,h_\phi\right]^2}$$

and $\Delta = \partial_\lambda x_p \partial_\phi y_p - \partial_\lambda y_p \partial_\phi x_p > 0$. Hence the velocity vector

$$\frac{\mathrm{d}\mathbf{R}}{\mathrm{d}t} = \mathbf{V} + \tilde{\boldsymbol{\Omega}} \times \mathbf{R}$$

can be written as $\mathrm{d}\mathbf{R}/\mathrm{d}t = u_p\widehat{\mathbf{x}}_p + v_p\widehat{\mathbf{y}}_p + w_p\widehat{\mathbf{H}}_p + \Omega r\cos\phi\,(T_1\widehat{\mathbf{x}}_p - T_2\widehat{\mathbf{y}}_p)$ where

$$u_p = h_x\frac{\mathrm{d}x_p}{\mathrm{d}t}\,, \qquad v_p = h_y\frac{\mathrm{d}y_p}{\mathrm{d}t}\,, \qquad w_p = \frac{\mathrm{d}H_p}{\mathrm{d}t}\,.$$

The map-projection equations reported in [18, 19] are obtained from eqs. (4.2), the formulas given in this appendix and the approximation $r = z_p + a \sim a$.

REFERENCES

[1] Dutton J. A., *The Ceaseless Wind: An Introduction to the Theory of Atmospheric Motion* (McGraw-Hill, New York) 1976, p. 176, 225.

[2] Gutman L. N., *Introduction to the Nonlinear Theory of Mesoscale Meteorological Processes* (Jerusalem, Israel Program) 1972, p. 3.

[3] Yih C.-S., *Stratified Flows* (Academic Press, New York) 1980, p. 1.

[4] Atkinson B. W., *Meso-scale Atmospheric Circulations* (Academic, London) 1981, p. 13.

[5] Pielke R. A., *Mesoscale Meteorological Modeling* (Academic Press, New York) 1984, pp. 17-21; 2nd edition (2002).

[6] Perkey D. J., *Formulation of mesoscale numerical models*, in *Mesoscale Meteorology and Forecasting*, edited by P. S. Ray (American Meteorological Society, Boston) 1986, pp. 575-579.

[7] Zeytounian R., *Asymptotic Modeling of Atmospheric Flows* (Springer, Berlin) 1990, p. 10, eqs. (2.31).

[8] Brown R. A., *Fluid Mechanics of the Atmosphere* (Academic Press, San Diego) 1991, p. 250, 254, eqs. (6.46), (6.57).

[9] Atkinson W. B., *Introduction to the fluid mechanics of meso-scale flow fields*, in *Diffusion and Transport of Pollutants in Atmospheric Mesoscale Flow Fields*, edited by A. Gyr and F.-S. Rys (Kluwer, The Netherlands) 1995, pp. 6,7, eqs. (1.1-2), and fig. 9.

[10] Eppel D. P. and Callies U., *Boundary conditions and treatment of topography in limited-area models*, in *Diffusion and Transport of Pollutants in Atmospheric Mesoscale Flow Fields*, edited by A. Gyr and F.-S. Rys (Kluwer, The Netherlands) 1995, p. 24, eqs. (2.1.1).

[11] Baines P. G., *Topographic Effects in Stratified Flows* (Cambridge University Press, Cambridge) 1995, p. 3.

[12] Durran D. R., *Numerical Methods for Wave Equations in Geophysical Fluid Dynamics* (Springer, New York) 1998, p. 16.

[13] Pielke R. A., *The status of mesoscale meteorological models*, in *Planning and Managing Regional Air Quality*, edited by P. A. Solomon and T. A. Silver (Pacific Gas & Electric Co. and Lewis Publishers, San Ramon, CA) 1994, pp. 435-463.

[14] Xue M., Droegemeler K. K., Wong V., Shapiro A. and Brewster K., *Advanced Regional Prediction System (ARPS) Version 4.0 User's Guide* (1995), pp. 119-120. http:// wwwcaps.ou.edu/ARPS/.

[15] Yamada T., *J. Meteorol. Soc. Jpn.*, **59** (1981) 108; Yamada T. and Bunker S., *J. Appl. Meteorol.*, **27** (1988) 562.

[16] McVittie G. C., *Quat. J. Mech. Appl. Math,* **1** (1948) 174; *J. Meteorol.*, **8** (1951) 161.

[17] Yamada T., Kao J. C.-Y. and Bunker S., *Atmos. Environ.*, **23** (1989) 539.

[18] Haltiner G. J., *Numerical Weather Prediction* (Wiley and Sons, New York) 1971, pp. 13-18.

[19] Haltiner G. J. and Williams R. T., *Numerical Weather Prediction and Dynamic Meteorology* (Wiley and Sons, New York) 1980, 2nd ed, pp. 6-14.

[20] Pielke R. A. *et al.*, *Meteorol. Atmos. Phys.*, **49** (1992) 69; *RAMS The Regional Atmospheric Modeling System Technical Description DRAFT*, http:// www.atmet.com/html/ docs/ rams_techman.pdf, section 2.2.

[21] Dudhia J., Gill D., Guo Y.-R., Hansen D., Manning K. and Wang W., *PSU/NCAR Mesoscale Modeling System Tutorial Class Notes and Users' Guide (MM5 Modeling System Version 2 with an introduction to version 3)* (1999), chapter 9, eqs. (1-4) and p. 9-5. http:// www.mmm.ucar.edu/ mm5/ mm5-home.html.

[22] Fast J. D. and Zhong S., *J. Geophys. Res.*, **103** (1998) 18927.

[23] *Pronóstico Numerico Regional (Modelo MM5)*, Servicio Meteorológico Nacional, http:// smn.cna.gob.mx/ productos/mm5/ htm/pag7773.htm

[24] Nuñez M. A., *Nuovo Cimento C*, **25** (2002) 13.
[25] GTOPO30 documentation, section 7, U. S. Geological Survey (1997). http:// www.scd.ucar.edu/ dss/datasests/ds758.0hmtl.
[26] Seignur C., Chinkin L. R., Morris E. R. and Kessler C. R., *Conceptual plan for air quality and meteorological modelling in the San Joaquin Valley*, in *Planning and Managing Regional Air Quality*, edited by P. A. Solomon and T. A. Silver (Pacific Gas & Electric Co. and Lewis Publishers, San Ramon, CA) 1994, pp. 46-47.
[27] Pedlosky J., *Geophysical Fluid Dynamics*, 2nd ed. (Springer, New York) 1987, p. 340.
[28] Holton J. R., *An Introduction to Dynamic Meteorology* 3rd ed. (Academic Press, San Diego) 1992, pp. 33-38.
[29] Cushman-Rosin B., *Introduction to Geophysical Fluid Dynamics* (Prentice Hall, New Jersey) 1994, p. 34.